

Numerical Study of Local Scour Around a Triangular Group of Circular Bridge Piers

Osama Rahim Shikh Hasan¹ , and Mustafa Günal² 

^{1,2}Department of Civil Engineering, Gaziantep University, Gaziantep, Türkiye

Correspondence should be addressed to Osama Rahim Shikh Hasan; osamarahim1989@gmail.com

Received: 28 July 2025

Revised: 13 August 2025

Accepted: 27 August 2025

Copyright © 2025 Made to Osama Rahim Shikh Hasan et al. This is an open-access article distributed under the Creative Commons Attribution License, which permits unrestricted use, distribution, and reproduction in any medium, provided the original work is properly cited.

ABSTRACT- Scour is a critical hydraulic phenomenon that undermines bridge foundations, leading to severe structural failures and significant economic losses. This study investigates the local scour behavior around triangular configurations of circular bridge piers through combined experimental testing in a laboratory flume and three-dimensional computational fluid dynamics (CFD) simulations using FLOW-3D. The experimental program was conducted in a recirculating flume (11.0 m × 0.756 m × 0.55 m) with uniform sediment (D₅₀ = 3.0 mm), varying the center-to-center spacing between the front pier and the two base piers across five non-dimensional spacing ratios (Z/B = 1.0, 3.5, 8.35, 15, 25) [1]. Numerical simulations were calibrated against experimental results for a single pier before extending to triangular group configurations under identical hydraulic and sediment conditions. Results shows that smaller Z/B ratios produce severe hydrodynamic interactions between piers, with merged scour holes and increased maximum scour depths (up to 100.5 mm at Z/B = 1.0). Findings from this study provide practical guidance for bridge design engineers, emphasizing the importance of pier spacing in mitigating scour risk in multi-pier arrangements.

KEYWORDS- Local Scour. Flow-3d, Triangular Group Configurations, Bridge Pier.

I. INTRODUCTION

Bridges are dynamic infrastructure components that ensure the continuity of transportation networks [2]. However, their foundations are susceptible to degradation from hydraulic processes, with local scour being one of the most prevalent and dangerous causes of failure [2][3][4][5]. Historical data indicate that scour has accounted for approximately 60% of bridge collapses in the United States since 1950, with catastrophic events such as the Schoharie Creek Bridge collapse in 1987 highlighting the potential for loss of life and major economic disruption [6]. This phenomenon happens, when water flows within the waterway considered as main reason for sediment transportation from the bed of river which causes the continue changes in the elevation of the bed-river over the waterway [7], this problem increasing as of the humane intervention like construction bridges on the rivers which causing reducing the river cross section that lead to increase the water flow velocity, the sediment transportation also increasing in the flow turbulence and creating downward vortexes started in the front face and continue to the bottom of the bridge elements like piers and

abutments, which eventually forming scour hole around bridge pier foundations [4][8][9][10][11], as shown in the Figure 1.



Figure 1: Scour hole around bridge pier [4]

While single-pier scour mechanisms have been extensively studied[3][12][13][14], bridge designs frequently employ grouped pier arrangements, including triangular configurations, to enhance structural stability[1]. These configurations alter the flow field significantly, introducing complex interactions between the vortices of adjacent piers. Triangular pier arrangements, in particular, combine direct flow impingement on the apex pier with partial wake shielding of the downstream base piers, creating a unique hydraulic environment that can either mitigate or intensify scour depending on the spacing between piers [15]. Previous experimental and numerical investigations by [16] [17] had demonstrated that reduced spacing intensifies turbulence, leading to deeper and more connected scour holes, while larger spacing can limit interference effects.

II. EXPERIMENTAL STUDY AND METHODOLOGY

The study employed a combined experimental and numerical approach to investigate local scour around triangular bridge pier configurations. The experimental phase was conducted in a recirculating flume the work was done by [1], the measuring 11.0 m in length, 0.756 m in width, and 0.55 m in depth, with transparent glass sidewalls and a steel base. The sediment bed consisted of uniform gravel with a median diameter (D₅₀) of 3.0 mm, a geometric standard deviation σ_g

= 1.2, and a bed thickness of 0.20 m. Flow discharge was maintained at 0.053 m³/s, yielding a mean velocity of 0.59 m/s, as shown in Figure 2.

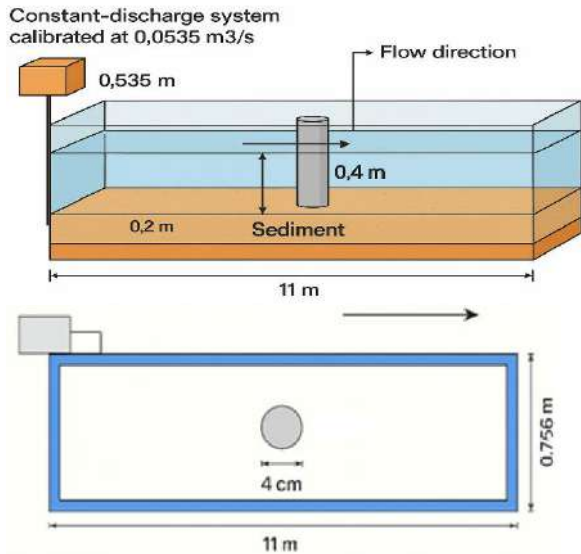


Figure 2: Drawing for illustration of experimental flume layout, geometry and dimensions wee the data from [1].

This study addresses this gap by integrating high-resolution laboratory measurements with calibrated CFD simulations using FLOW-3D to evaluate how variations in the Z/B ratio influence scour depth, bed morphology, and flow structures in triangular pier groups. where Z is the vertical distance between the middle of the base piers line and the head forwarding pier. and b is the pier diameter (4.0 cm). As shown in Figure 3. The results aim to inform both design practice and future research on scour mitigation for multi-pier systems. Five models of triangular group piers will next be simulated to represent a triangular pier group configurations following the successful calibration of the numerical model with a single-pier. In this configuration the head forwarding to facing the upstream flow. These five cases are chosen to examine how changes of the pier spacing affect the flow behavior around the group of piers and their influence on local scour depth development as shown in Table 1 and Figure 3.

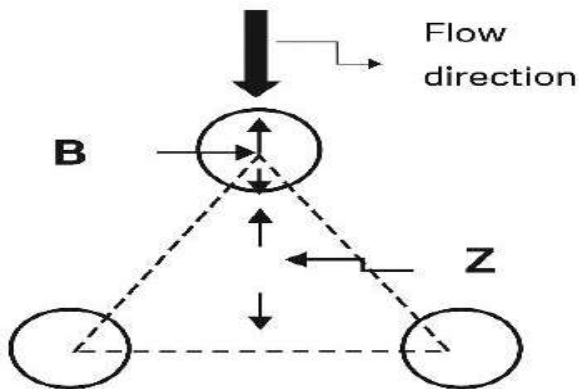


Figure 3: Illustration of triangular of group of pier configuration

These models differ only in the center-to-center distance

between the front and base piers, defined by the non-dimensional ratio Z/b, where Z is the vertical distance between the middle of the base piers line and the head forwarding pier. and b is the pier diameter (4.0 cm). As shown in Figure 4.

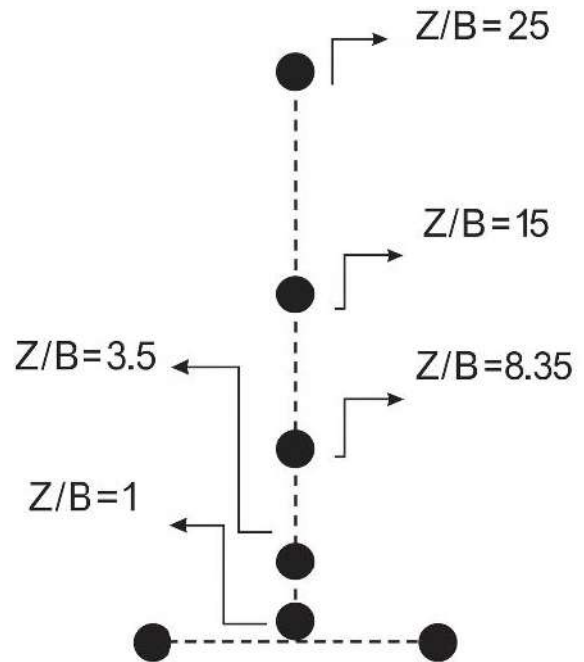


Figure 4: Illustration of pier spacing.

The selected of Z/b (ranging from 1 to 25) were chosen to reflect a wide range of hydrodynamic interaction scenarios, from strong interference at close spacing to near isolated or isolated behavior at wide spacing.

Table 1: Simulation Scenarios

Model	Z/b Ratio	Z (cm)	B (cm)
Model 0	-	-	-
Model 1	1.00	4.0	4
Model 2	3.5	14.0	4
Model 3	8.45	33.4z	4
Model 4	15.0	60.0	4
Model 5	25.0	100.0	4

The numerical simulation of local scour around cylindrical bridge piers in this study was conducted using FLOW-3D, a computational fluid dynamics (CFD) software capable of modeling free-surface flows and sediment transport [3][18][19].

The main Equations for Scour Simulation in FLOW-3D that used to simulation of local scour around bridge piers is based on a set of well-established sediment transport equations. The Shields parameter and its critical value (Soulsby–Whitehouse, 1997) define the threshold for sediment motion [20], while bedload transport equations (Nielsen, Meyer-Peter & Müller type) and suspended load formulations (van Rijn, 1984) quantify the rate of sediment movement [21][22][23]. The settling velocity of particles [20][24]. To maintain bed stability, the angle of repose/avalanching model redistributes material when slopes exceed the critical angle, and an entrainment function controls the rate of sediment pickup. Together, these equations provide a comprehensive framework for representing scour initiation, sediment transport, and bed deformation around bridge piers.

However the main equations for scour simulation in FLOW-3D mentioned in details in [18][25][26]. The methodology began with validating the model against experimental data for a single pier case (Model 0) before extending to simulations of triangular pier group configurations. Key physical processes were captured by activating relevant modules such as sediment scour modeling, gravity, fluid viscosity, and turbulence. Gravity was set to -9.81 m/s^2 in the vertical direction, and fluid density was computed dynamically. The computational domain replicated the experimental flume, featuring a 3 m long and 0.2 m thick sediment bed, with a vertical cylindrical pier (4 cm diameter, 0.4 m height) embedded 20 cm into the bed. A structured mesh with 2 cm resolution, refined to 1 cm near the pier, yielded around 128,000 cells, balancing accuracy and computational efficiency. Boundary conditions included a discharge inlet of $0.053 \text{ m}^3/\text{s}$ at the upstream end, a free outlet downstream, no-slip sidewalls and bed, and a pressure boundary at the top to simulate the free surface. The initial water depth was set to 12 cm above the sediment bed. Sediment was modeled as a non-cohesive material with a median grain size of 3 mm, specific gravity of 2.65, and a bulk density of 2650 kg/m^3 , with both bedload and suspended load transport mechanisms activated to fully capture sediment dynamics during scour development. Model calibration was conducted using FLOW-3D by replicating the experimental conditions for a single cylindrical bridge pier (Model 0). The numerical domain and input parameters, including flow, geometry, and sediment properties, were matched with the laboratory setup to ensure accurate simulation of equilibrium scour. Calibration relied on applying validated sediment transport equations such as the Soulsby-Whitehouse and Nielson formulas. A summary of the main numerical run conditions used in the calibration is

provided in Table 2.

Table 2: input parameter

Parameter	Value
Domain Dimensions (L×W×H)	11.0×0.756×0.55 m
Sediment Layer Thickness	0.20 m
Water Flow Depth	0.12 m
Discharge	$0.0535 \text{ m}^3/\text{s}$
Mean Flow Velocity	0.59 m/s
Pier Diameter	0.04 m
Pier Height	0.40 m
Grain Size (d_{50})	0.003 m
Sediment Density	2650 kg/m^3
Critical Packing Fraction	0.64
Shields Parameter	Auto-calculated
Bed Roughness / d_{50} Ratio	2.5
Entrainment Coefficient	0.018
Bed Load Coefficient	12

As shown in Figure 5, the relationship between the experimental (EXP) and numerical (CFD) results showed a nearly one-to-one correspondence across the different recorded time intervals. This indicates that the CFD model successfully captured the governing hydraulic and sediment transport processes. $R^2 = 0.97$ confirms the reliability of the calibration, reflecting that approximately 97% of the variability in the experimental results was explained by the numerical model. Such a high level of correlation validates the numerical assumptions and parameterization adopted in the simulations, including sediment transport coefficients, bed roughness scaling, and Shields parameter calculations.

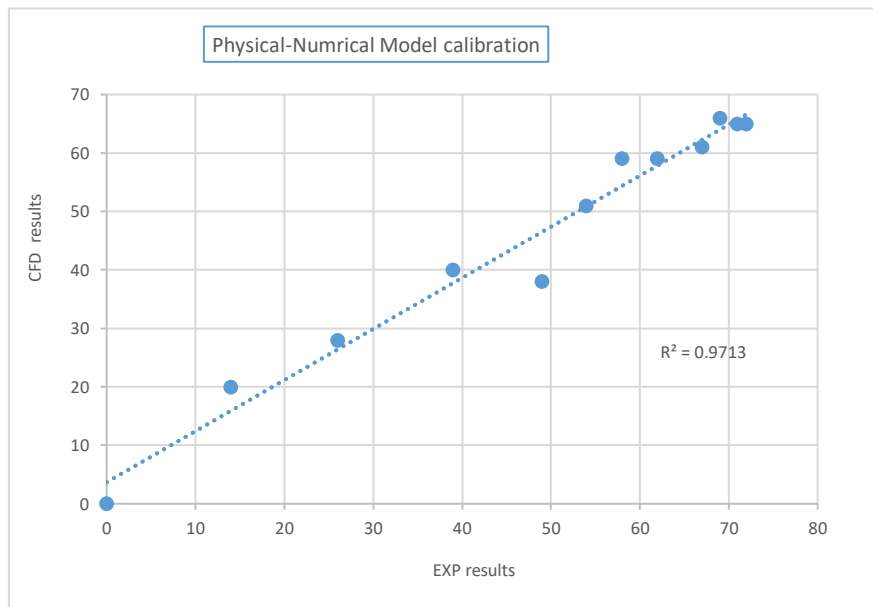


Figure 5: Experimental and Numerical Model (Model 0) Calibration.

III. RESULTS AND DISCUSSION

The results highlight the significant influence of pier spacing on scour development and flow structure. At $Z/B = 1.0$, intense hydrodynamic interference between the piers resulted in a fully merged scour hole, with a maximum depth

of 100.5 mm at the apex pier and nearly equivalent depths at the base piers. The velocity field exhibited jet-like accelerations between piers and strong horseshoe vortices at all pier bases.

The numerical results clearly demonstrate that the spacing ratio (Z/B) strongly influences scour depth, flow structure,

and bed morphology around triangular grouped bridge piers. At $Z/B = 1.0$, the extremely close spacing produced severe flow contraction, strong jet-like acceleration, and highly intense horseshoe vortices, resulting in a fully merged scour hole with maximum depth exceeding 100 mm at the front pier. For $Z/B = 3.5$, interaction remained significant, though slightly weaker, with partially merged scour holes and reduced depths (front ≈ 92 mm, rear ≈ 78 – 81 mm). At $Z/B = 8.35$, the wider spacing allowed partial flow recovery, leading to distinctly separated scour holes connected by shallow troughs, with maximum depths reduced further (front ≈ 88 mm, rear ≈ 69 – 70 mm). When the spacing increased to $Z/B = 15$, the flow fields became nearly independent, and scour holes were well separated, symmetrical, and shallower (front ≈ 92 mm, rear ≈ 78 – 81 mm), indicating quasi-isolated pier behavior. Finally, at $Z/B = 25$, the piers behaved as fully isolated structures with no measurable hydraulic interference; each pier developed its own scour hole independently, with depths of about 92–96 mm at the front and 90–92 mm at the rear.

A. Flow Dynamics

At $Z/B = 1.0$, the close spacing produced severe contraction

and jet-like acceleration, generating strong horseshoe vortices and intense wake turbulence that directly impacted all three piers.

At $Z/B = 3.5$, contraction effects were slightly weaker but still caused significant flow interaction and turbulence transfer toward the rear piers. With $Z/B = 8.35$, flow recovery became more evident, and hydraulic interference was reduced, with only partial overlap of wakes.

At $Z/B = 15$, the flow fields were mostly independent, with minimal interaction between the front and rear piers. Finally, at $Z/B = 25$, each pier behaved hydraulically independently, with isolated stagnation zones, vortices, and velocity fields. Furthermore, the velocity field as shown in Figure 6 and Figure 7, the localized acceleration velocity field around the front and rear piers, clearly shows concentrated high-velocity streaks between the piers. These high-energy going into the wake region, where large-scale turbulence controls. Immediately at the base of the front pier, a strong horseshoe vortex system forms, wrapping around the pier and scouring sediment from its base. Behind the front pier, the wake interacts almost instantly with the two rear piers, producing secondary horseshoe vortices and wake vortices that intensify sediment removal around them.

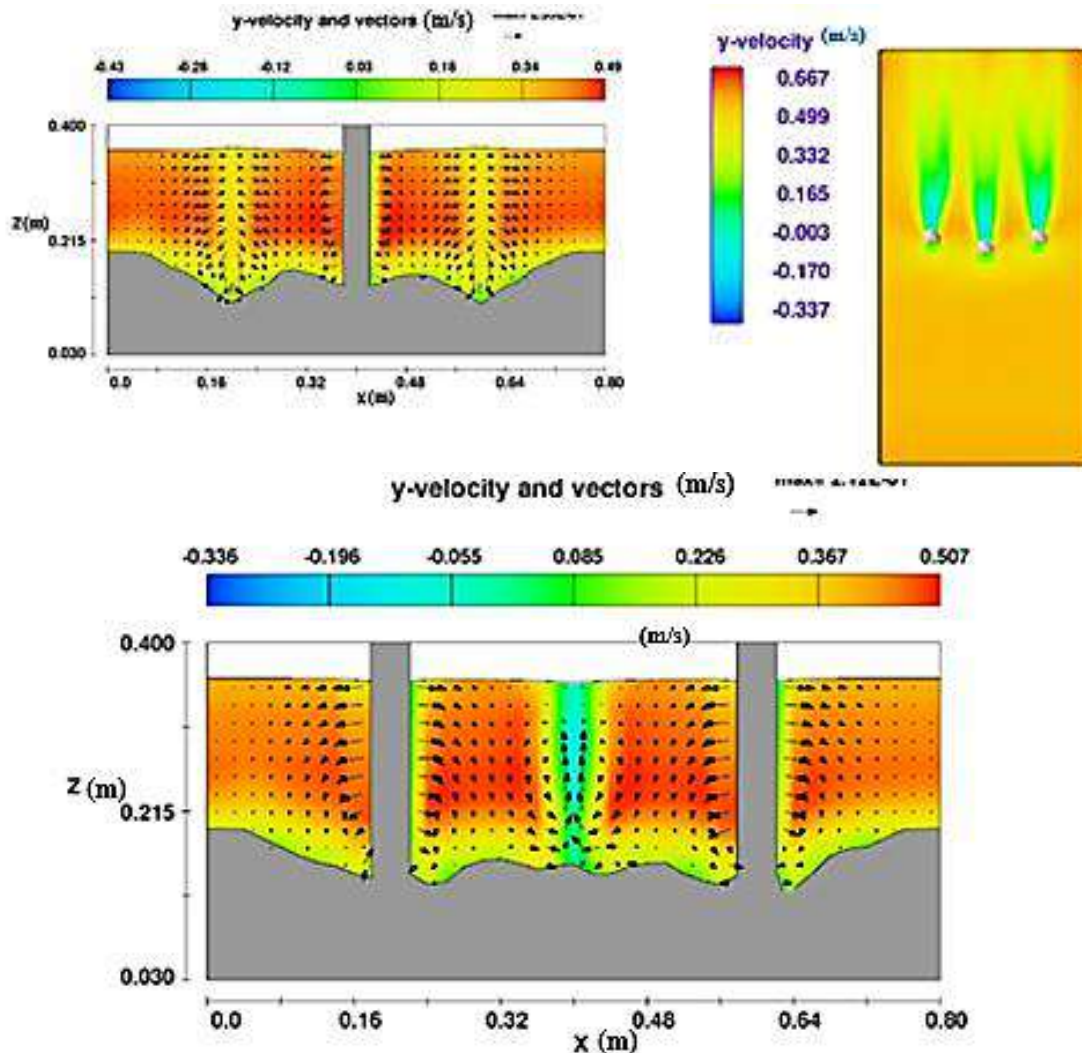


Figure 6: The local acceleration velocity field around the front and rear piers

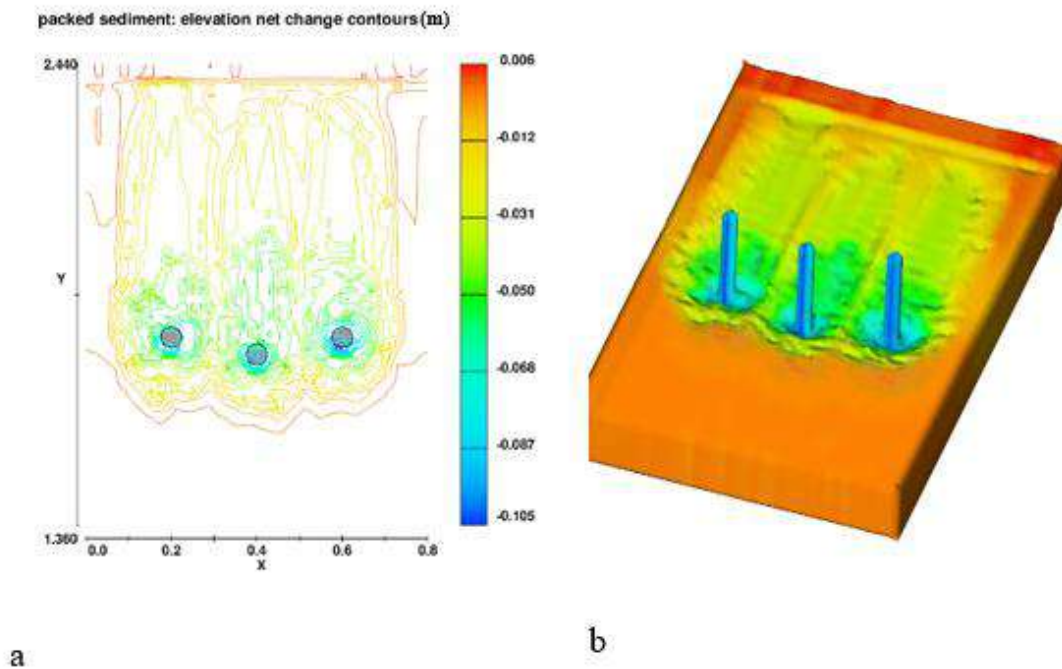


Figure 7: Scour holes and changed bed profile

B. Temporal Development of Scour

In all cases, scour developed rapidly during the early phase and slowed as equilibrium was approached. At $Z/B = 1.0$, the scour grew very quickly in the first 30 minutes before stabilizing. At $Z/B = 3.5$, the scour developed slightly more gradually, reaching equilibrium within ~50–60 minutes. At

$Z/B = 8.35$, the process was slower, with moderate deepening rates before stabilization. At $Z/B = 15$, the front pier showed faster early scour, while the rear piers stabilized earlier due to weaker interference. At $Z/B = 25$, the scour-time curves for all piers were nearly parallel, confirming independent development, with a rapid initiation phase followed by gradual stabilization at equilibrium as shown in Figure 8.

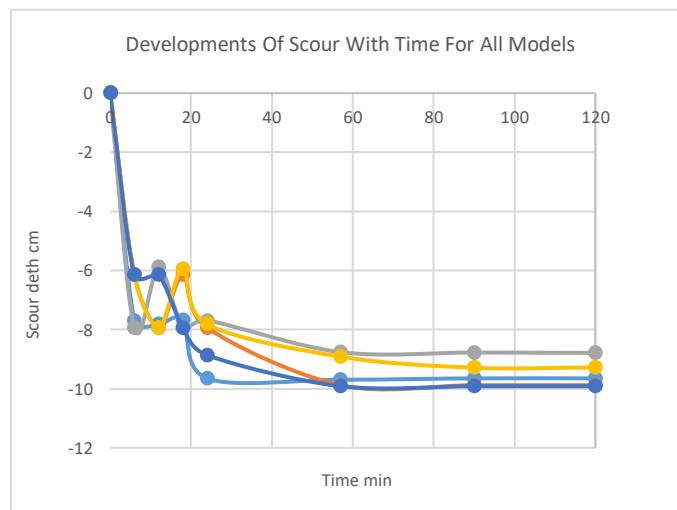


Figure 8: Developments of scour with time for all models

IV. CONCLUSION

The investigation has demonstrated that pier spacing plays a decisive role in determining both the severity and the spatial distribution of local scour. In tightly spaced arrangements, such as $Z/B \leq 3.5$, the hydraulic behaviours of the group are dominated by strong contraction effects and wake interactions. The apex pier generates intense horseshoe vortices, and the narrow gaps channel high-energy jets directly toward the rear piers. This interaction leads to fully

or partially merged scour holes, with depths at the rear piers approaching those at the front. When the spacing is increased to intermediate values, particularly in the range of $Z/B \approx 8.35-15$, the flow has more opportunity to recover between piers. The wakes lose some of their energy before reaching downstream piers, resulting in scour holes that are more distinct and less deep at the rears. The apex still tends to exhibit the largest scour depth due to direct impact from the oncoming flow, but the reduction in

rear-pier scour is significant, and the risk of simultaneous undermining across the group is much lower.

At the widest spacing, represented by $Z/B = 25$, the piers behave hydrodynamically as isolated structures. Each pier forms its own horseshoe vortex and wake, and scour development is governed almost entirely by local approach conditions rather than by interactions with other piers. Although scour depths can still be substantial—sometimes even greater at a rear pier due to localized velocity biases—the absence of interaction means the problem is localized to individual foundations rather than affecting the entire group. A consistent pattern emerged in the temporal evolution of scour across all configurations: the most rapid bed lowering occurred during the initial phase of exposure to the flow, followed by a more gradual approach to equilibrium. This early stage was most intense in the tightly spaced cases, highlighting their vulnerability during short-duration high-flow events such as flood peaks.

Overall, the study confirms that while wide spacing effectively eliminates compound scour interaction, intermediate spacing offers a practical balance between structural compactness and scour risk reduction, and tight spacing requires more aggressive and comprehensive protective measures.

CONFLICTS OF INTEREST

The authors declare that they have no conflicts of interest.

REFERENCES

- Anand, A. and M. Beg, "Local scour at group of bridge piers founded in gravel bed in staggered arrangement," *Results in Engineering*, vol. 23, p. 102608, 2024. Available from: <https://doi.org/10.1016/j.rineng.2024.102608>
- Tan, J.-S., et al., "Lessons learnt from bridge collapse: A view of sustainable management," *Sustainability*, vol. 12, no. 3, p. 1205, 2020. Available from: <https://doi.org/10.3390/su12031205>
- Alasta, M.S., et al., "Modeling of Local Scour Depth Around Bridge Pier Using FLOW 3D." Available from: <https://tinyurl.com/v9fve5t8>
- Melville, B.W. and S.E. Coleman, *Bridge scour*. Water Resources Publication, 2000. Available from: <https://tinyurl.com/ytede8jm>
- Bettess, R., "A review of predictive methods for general scour," in *First International Conference on Scour of Foundations (ICSF-1)*, Texas A&M University, College Station, Texas, USA, 2002. Available from: <https://core.ac.uk/download/pdf/326240538.pdf>
- Pagán-Ortiz, J.E., "Impact of the federal highway administration's scour evaluation program in the United States of North America's highway bridges," in *First International Conference on Scour of Foundations*, College Station, USA, Nov. 17–20, 2002. Available from: <https://core.ac.uk/download/pdf/326239249.pdf>
- Koursari, E., et al., "Monitoring of infrastructure at risk of scour and other hydraulic actions," in *EGU General Assembly Conference Abstracts*, 2024. Available from: <https://tinyurl.com/bdzhx6tk>
- Melville, B.W. and A.J. Raudkivi, "Flow characteristics in local scour at bridge piers," *Journal of Hydraulic Research*, vol. 15, no. 4, pp. 373–380, 1977. Available from: <https://doi.org/10.1080/00221687709499641>
- Ettema, R., *Scour at bridge piers*, 1980. Available from: [https://doi.org/10.1061/\(ASCE\)0733-9429\(1985\)111:4\(713\)](https://doi.org/10.1061/(ASCE)0733-9429(1985)111:4(713))
- Niederoda, A. and C. Dalton, "A review of the fluid mechanics of ocean scour," *Ocean Engineering*, vol. 9, no. 2, pp. 159–170, 1982. Available from: [https://doi.org/10.1016/0029-8018\(82\)90011-7](https://doi.org/10.1016/0029-8018(82)90011-7)
- Khawairakpam, P. and A. Mazumdar, "Local scour around hydraulic structures," *International Journal of Recent Trends in Engineering*, vol. 1, no. 6, p. 59, 2009. Available from: <https://tinyurl.com/yc28nen7>
- Dheyab, A.S. and M. Günal, "Experimental investigation of local scour depth around cylindrical bridge piers in non-cohesive sediments at near-threshold velocity for sand." Available from: <https://tinyurl.com/ycyr9jw5>
- Ismael, A., M. Gunal, and H. Hussein, "Effect of bridge pier position on scour reduction according to flow direction," *Arabian Journal for Science and Engineering*, vol. 40, no. 6, pp. 1579–1590, 2015. Available from: <https://link.springer.com/article/10.1007/s13369-015-1625-x>
- Omara, H. and A. Tawfik, "Numerical study of local scour around bridge piers," in *IOP Conference Series: Earth and Environmental Science*, IOP Publishing, 2018. Available from: <https://tinyurl.com/uae9ub7n>
- Ahmad, N., et al., "Three-dimensional CFD modeling of wave scour around side-by-side and triangular arrangement of piles with REEF3D," *Procedia Engineering*, vol. 116, pp. 683–690, 2015. Available from: <https://doi.org/10.1016/j.proeng.2015.08.355>
- Akhlaghi, E., et al., "Assessment the effects of different parameters to rate scour around single piers and pile groups: a review," *Archives of Computational Methods in Engineering*, vol. 27, no. 1, pp. 183–197, 2020. Available from: <https://link.springer.com/article/10.1007/s11831-018-09304-w>
- Heidarpour, M., H. Afzalimehr, and E. Izadinia, "Reduction of local scour around bridge pier groups using collars," *International Journal of Sediment Research*, vol. 25, no. 4, pp. 411–422, 2010. Available from: [https://doi.org/10.1016/S1001-6279\(11\)60008-5](https://doi.org/10.1016/S1001-6279(11)60008-5)
- Flow Science, Inc., *FLOW 3D User Manual*, Version 2008. Available from: <https://doi.org/10.1002/wrcr.20442>
- Ghasemi, M. and S. Soltani-Gerdefaramarzi, "The scour bridge simulation around a cylindrical pier using Flow-3D," *Journal of Hydrosocieties and Environment*, vol. 1, no. 2, pp. 46–54, 2017. Available from: https://jhe.usb.ac.ir/article_3357.html
- Soulsby, R. and R. Whitehouse, "Threshold of sediment motion in coastal environments," in *Pacific Coasts and Ports '97: Proceedings of the 13th Australasian Coastal and Ocean Engineering Conference and the 6th Australasian Port and Harbour Conference*, vol. 1, Centre for Advanced Engineering, University of Canterbury, Christchurch, NZ, 1997. Available from: <https://tinyurl.com/44dbtcs7>
- Dey, S., "Bedload Transport," in *Fluvial Hydrodynamics: Hydrodynamic and Sediment Transport Phenomena*, Springer, 2024, pp. 379–461. Available from: https://link.springer.com/chapter/10.1007/978-3-031-26038-4_5
- Wiberg, P.L. and J. Dungan Smith, "Model for calculating bed load transport of sediment," *Journal of Hydraulic Engineering*, vol. 115, no. 1, pp. 101–123, 1989. Available from: [https://doi.org/10.1061/\(ASCE\)0733-9429\(1989\)115:1\(101\)](https://doi.org/10.1061/(ASCE)0733-9429(1989)115:1(101))
- Van Rijn, L.C., "Sediment transport, part I: bed load transport," *Journal of Hydraulic Engineering*, vol. 110, no. 10, pp. 1431–1456, 1984. Available from: [https://doi.org/10.1061/\(ASCE\)0733-9429\(1984\)110:10\(1431\)](https://doi.org/10.1061/(ASCE)0733-9429(1984)110:10(1431))
- Damgaard, J.S., R.J. Whitehouse, and R.L. Soulsby, "Bed-load sediment transport on steep longitudinal slopes," *Journal of Hydraulic Engineering*, vol. 123, no. 12, pp. 1130–1138, 1997. Available from: [https://doi.org/10.1061/\(ASCE\)0733-9429\(1997\)123:12\(1130\)](https://doi.org/10.1061/(ASCE)0733-9429(1997)123:12(1130))
- Flow Science, Inc., *FLOW-3D® Version 12.0 Users Manual (2018)*, FLOW-3D [Computer software], Santa Fe, NM, 2018.
- Wei, G., et al., "The sedimentation scour model in FLOW-3D®," *Flow Science Report*, vol. 3, pp. 1–29, 2014. Available from: <https://tinyurl.com/47s4dw3p>